PROCEEDINGS OF SCIENCE

Comprehension of AmBe+BGO source to calibrate neutron tagging in electron antineutrino physics

Takatomi Yano,[a,*] **Hiroshi Ito,**[b] **Masaki Ishitsuka,**[b] **Yota Hino,**[c] **Masayuki Harada,**[c] **Akihiro Minamino**[d] **and Ryo Shibayama**[d]

[a] *Kamioka Observatory, ICRR, The University of Tokyo, 456 Mozumi, Kamioka, Hida, Gifu, Japan*

[b] *Department of Physics, Faculty of Science and Technology, Tokyo University of Science, Noda, Chiba, Japan*

[c] *Department of Physics, Okayama University, Okayama, Japan*

[d] *Department of Physics, Yokohama National University, Yokohama, Kanagawa, Japan*

E-mail: tyano@km.icrr.u-tokyo.ac.jp

Massive neutrino detector experiments, which are oriented for the electron antineutrino observation, calibrate their neutron tagging efficiency using AmBe neutron sources. Super-Kamiokande, a large water Cherenkov detector experiment, also started their new experimental phase SK-Gd for the astrophysical antineutrino observation. In their calibration, AmBe neutron source applied used with surrounding BGO scintillator crystals. The neutron emission is triggered and identified by scintillation light emission of 4438 keV gamma-ray from the source, and thus the neutron tagging efficiency is evaluated. Super-Kamiokande reports a relative 10% inconsistency between the efficiency value of the simulation and measurements. The reason should be investigated rapidly, and a sideband study was started to measure neutron and gamma rays from the AmBe source. In the presentation, the progress of measurements will be reported as follows: energy spectrum measurements for neutron with gamma-ray emission based on time-of-flight, emission ratio of the neutron with/without gamma-ray.

38th International Cosmic Ray Conference (ICRC2023)
26 July - 3 August, 2023
Nagoya, Japan

ICRC2023
38th International Cosmic Ray Conference
The Astroparticle Physics Conference

*Speaker

PoS(ICRC2023)1067

1. Introduction

Americium-Beryllium (AmBe) source is a famous calibration source of neutron, accompanying 4438 keV γ-ray emission. It is commonly used as a calibration source for large neutrino detector experiments, to evaluate their performance to detect neutrons. The evaluation is done by coincidental detection of the immediate γ-ray event and the delayed neutron event, which occurs after neutron thermalization and capture on the nuclei. Their neutron tagging technique is essential to identify the electron antineutrino ($\bar{\nu}_e$) interaction, $\bar{\nu}_e + p \rightarrow e^+ + n$.
Recently, Super-Kamiokande experiment (SK) started their new experimental phase with gadolinium-loaded water (SK-Gd). In SK-Gd phase, neutron tagging technique plays critical role to improve the observation sensitivity, e.g., the search for diffused supernova neutrino background [1]. SK applied their AmBe source to evaluate their neutron detection and reported relative ~10% discrepancy of neutron tagging efficiency between the data and the simulation [2]. The AmBe source was deployed with BGO scintillators, which potentially affect the evaluation through neutron interaction in the BGO. In this paper, we report our experimental approach to evaluate the characteristics of the AmBe source. More details are described and available in a reference [3]. The knowledge about the characteristics of one's own AmBe source will be valuable to understand this kind of discrepancy and to improve the detector calibration, not only for SK but also further neutrino experiments.

2. Americium-Beryllium source

Americium-Beryllium source is composed of ^{241}Am and ^{9}Be and emits neutrons according to the following chain reaction: $^{241}\mathrm{Am} \rightarrow {}^{237}\mathrm{Np} + \alpha$, $^{9}\mathrm{Be} + \alpha \rightarrow {}^{12}\mathrm{C}^{*}$ (or ^{12}C) + n. In this process, the carbon nucleus can adopt several excited states, although only the first excited state emits γ-rays. The characteristics of the neutrons, i.e., the energy spectrum, flux, and emission ratio of neutrons and γ-rays, are correlated to the ratio of these ^{12}C excited states. The neutron energy spectra below 2.5 MeV can be different between each AmBe source products [4]. This difference is attributed to the structure or the production method of the source. There are theoretical and experimental studies about the neutron energy spectra from the AmBe source, and its correlation between the excited states of ^{12}C [4–7]. Figure 1 shows measured energy spectra [6, 8, 9] and our model, which is applied for our Monte-Carlo simulation and analysis. In this model, each neutron energy spectrum is paired with the excited states of ^{12}C. We adopted the International Standard ISO-8529-1:2001(E) to model the total neutron spectrum [8], and divided into three parts based on the theoretical predictions of De Guarrini and Malaroda [5]. These partial neutron spectra are correlated with the states of ^{12}C: ground state (n_{GND}), first excited state ($n_{1\mathrm{st}}$), and the second or higher excited states ($n_{2\mathrm{nd}}$).

Most of the neutrons are paired with the first excited state ($n_{1\mathrm{st}}$) and the ground state (n_{GND}) of ^{12}C nucleus. The first excited state immediately emits a γ-ray with its excitation energy of 4438 keV and relaxes to the ground state. Neutrons paired with the second excited state of carbon ($n_{2\mathrm{nd}}$) also significantly contribute to the energy spectra. The second excited state of ^{12}C, with an energy of 7654 keV decays by emitting three α-particles with a probability of ~99.6%, and only ~0.4% of the state decays by emitting two γ-rays (energy: 3215 and 4438 keV) [10]. There is negligibly small probability that these decay alpha particles interact with ^{9}Be subsequently and emits

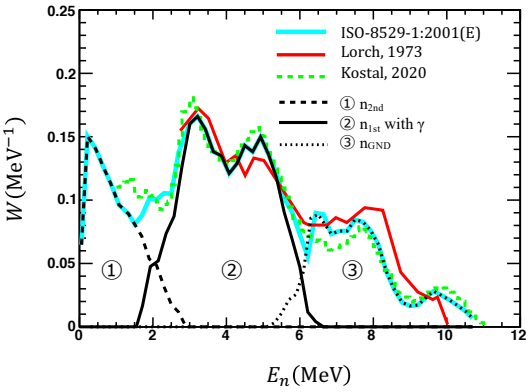

Figure 1: Measured neutron energy spectra of an AmBe source based on ISO 8529-1:2001(E) [8], E. Lorch [6], and M. Kostal et al. [9]. These measurements are conducted without considering the excited states of ^{12}C. n_{GND}, $n_{1\mathrm{st}}$, and $n_{2\mathrm{nd}}$ represent the partial neutron spectra with the following states of ^{12}C: ground state, first excited state, and second or higher excited states, respectively.

coincidental 4438 keV γ-ray and neutron. Finally, break-up neutrons paired with higher excited states, accompanying no γ-ray, are combined and treated as $n_{2\mathrm{nd}}$ in the following discussion [4].

3. Experimental Approach

In this section, we report the measurement of following characteristics for comprehensive understanding of our AmBe source.

- Neutron yield, total neutron emission rate ($n_{\mathrm{GND}} + n_{1\mathrm{st}} + n_{2\mathrm{nd}}$)
- $n_{1\mathrm{st}}$ emission rate
- $n_{1\mathrm{st}}$ energy spectrum
- Ratio of n_{GND} and $n_{1\mathrm{st}}$ emission

Our AmBe source is supplied by Kamioka observatory, Institute for Cosmic Ray Research, The University of Tokyo, Japan. It is produced by the French Alternative Energies and Atomic Energy Commission (CEA) before the early 1990s. ^{241}Am, with the strength of 97 μCi, is encapsulated with ^{9}Be in a stainless cylinder with outer diameters of 12.5 mm and a height of 12.5 mm.

3.1 Neutron yield measurement

The neutron yield was measured in March 2022 by the National Institute of Advanced Industrial Science and Technology (AIST), Japan. The measurement is done by comparing with the national standard field of thermal neutrons at AIST in the same condition, which is AmBe (standard) source located in a graphite pile. Thermal neutron counting was done with a ^{3}He proportional counter [11]. The neutron yield was given as $236.8 \pm 5.0\, n \cdot \mathrm{s}^{-1}$ (S_n).

3.2 Measurement of $n_{1\mathrm{st}}$ emission rate

As discussed in Section 2, $n_{1\mathrm{st}}$ emission always accompanies 4438 keV γ-ray emission. Thus, the intensity of $n_{1\mathrm{st}}$ can be evaluated by that of the γ-ray. Here, the intensity of 4438 keV γ-ray

was measured using a high-purity Ge (HPGe) detector (ORTEC, GEM110P4-ST). The detection efficiency was estimated with a ^{60}Co calibration source (19.5 kBq) and Geant4-based Monte Carlo simulations. Figure 2 (a) and (b) show the energy spectra obtained from our AmBe source; the spectra measurements were performed at distances of 10 and 50 mm from the surface of the HPGe detector, respectively. The FWHM of 4438 keV γ-ray peak is 119 keV at L = 10 mm, and 114 keV at L = 50 mm. They are consistent and explained well with the Doppler broadening at AmBe source [12]; The measured intensity of the 4438-keV γ-ray was 110.1 ± 15.5 γ/s (S_γ).

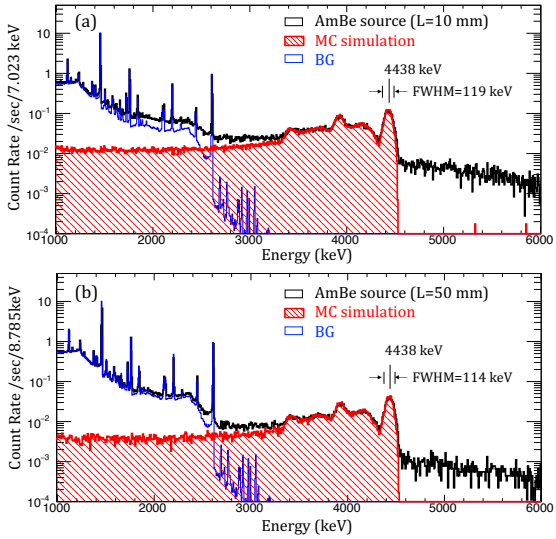

Figure 2: Energy spectrum of an AmBe source (black) and background (blue) measured using an HPGe detector, and the simulated spectrum of 4438-keV γ-rays emitted from the AmBe source (red). (a) 10 mm and (b) 50 mm distance between the center of the AmBe source and the HPGe surface

3.3 Measurement of n_{1st} energy spectrum

To determine the kinetic energy spectrum of n_{1st} neutrons, we used the time-of-flight method, in which the neutron kinetic energy is measured by the difference between the arrival times of the neutrons and the γ-ray. A NaI(Tl) inorganic scintillator detector (NaI), with the scintillator size of 51 mm × 51 mm × 152 mm, and a Saint-Gobain BC501A liquid scintillator detector (LS) are used for the measurement. The shape of the liquid scintillator was cylinder with the diameter of 76 mm and the height of 76 mm. These scintillators are both connected to photomultiplier tubes. The output signal waveforms are recorded by an oscilloscope (Lecroy, 100MXi).
For the measurement, the NaI detector, LS detector and the AmBe source were arranged in a line. The source was placed nearby the NaI, and its center was at a distance of 63.21 cm from that of LS. The n_{1st} neutron events were identified by coincidental detection of neutron in the LS and 4438 keV γ-ray photoelectric peak detection in the NaI. The neutron and γ-ray background signals in the LS were distinguished via pulse-shape discrimination (PSD) method.

The neutron arrival-time distribution is shown in Figure 3 (a). The black solid and red dashed histograms represent the experimental data and the simulation based on our n_{1st} partial spectrum model, respectively. Then, based on the time of flight, the neutron kinetic energy is calculated with the arrival time difference between the NaI(Tl) and LS detectors, given as

$$E_{\mathrm{TOF}} = m_n \left(\frac{1}{\sqrt{1-(L/ct)^2}} - 1 \right), \tag{1}$$

where m_{n} is the neutron mass, L is the path length of the neutron (63.21 cm), and ct is the path length of light during flight.

The measured neutron energy spectra and the expectations from the simulation are shown in Figure 3 (b). The red band indicates systematic uncertainty of the simulation, which is dominated by the difference of the neutron cross-section data sets. In comparison with the simulation, $\chi^2/dof = 28.7/40$ is calculated, which corresponds to the p-value of 0.908. This value represents that the obtained energy spectrum is in good agreement with the predicted model.

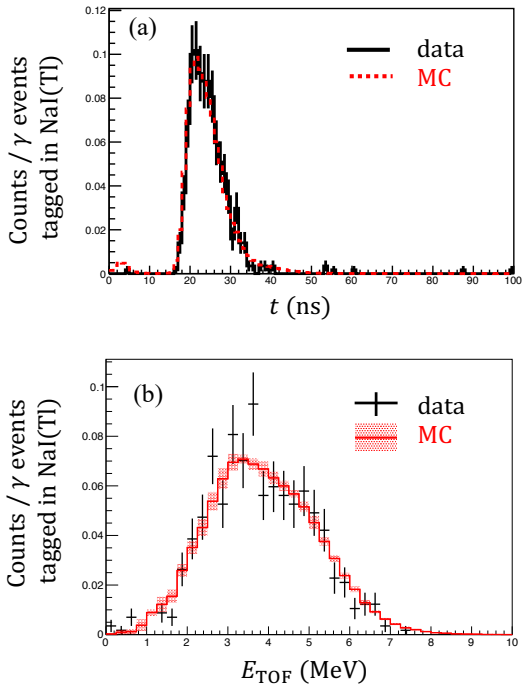

Figure 3: Arrival time distribution (a) and neutron energy spectra of data and simulation based on time-of-flight (b). Both events are selected by requiring neutron identified by PSD of the liquid scintillation detector and γ detection in the NaI(Tl) detector. The black dots and red lines are data and the simulation, respectively.

3.4 Measurement of n_{GND} and $n_{1\mathrm{st}}$ emission ratio

The measurement of neutron emission ratio $R_{n0/n1}$, which is the ratio of the intensity of n_{GND} to that of $n_{1\mathrm{st}}$, is described in this section. Single NaI(Tl) detector is supplied for this measurement, as shown in Figure 4. The distance (L) between the centers of the AmBe source and the NaI(Tl) detector was varied from 3.5 to 38.5 cm. The distribution of the visible energy for each distance is shown in Figure 5. The high-energy tail above 4438 keV γ-ray peak is understood as the contribution of the neutrons from the source. A part of neutrons interacts with and excites nuclei in the NaI(Tl) detector (inelastic scattering). The de-excitation γ-rays from these nuclei are detected by its energy

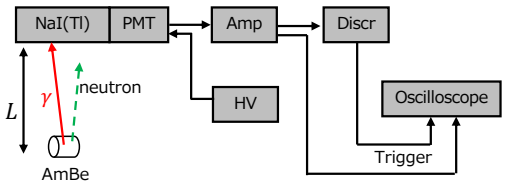

Figure 4: Schematics of experimental setups.

deposition and scintillation in the detector. Neutrons also recoil the nuclei without the excitation, but this elastic scattering process (nuclear recoil) has smaller energy deposition by an order of magnitude. This neutron inelastic scattering process is utilized to evaluate the emission ratio of n_{GND} and $n_{1\mathrm{st}}$, considering the different acceptance for single neutron (n_{GND}) detection ($\propto L^{-2}$) and for coincidental detection of neutron ($n_{1\mathrm{st}}$) and γ-ray ($\propto L^{-4}$).
A ratio of high-energy tail ($E_{\mathrm{vis}} > 5$ MeV) to the 4438 keV peak, $R_{\mathrm{tail/peak}}$, is given as

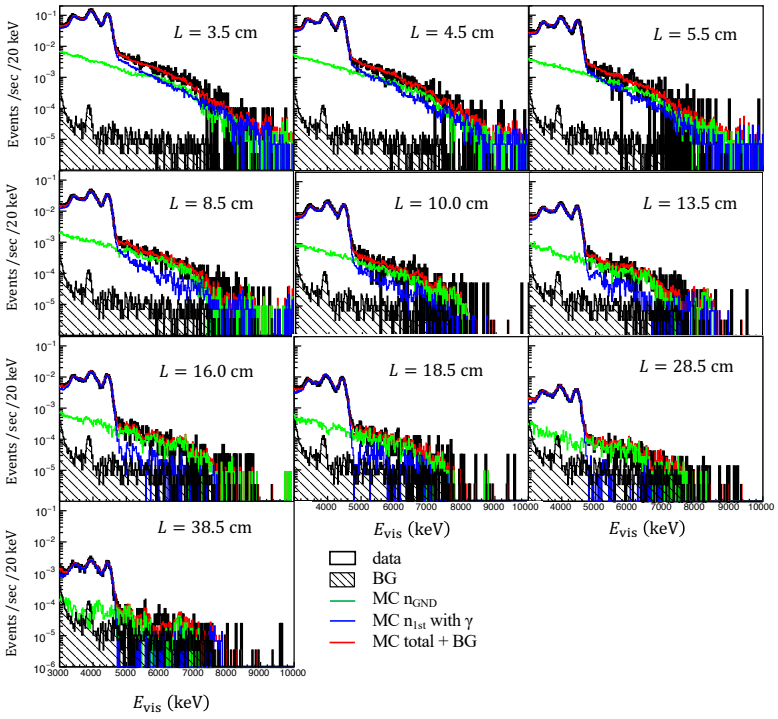

Figure 5: Distribution of visible energy in the NaI(Tl) detector for a distance between the center of the AmBe source and the NaI(Tl) detector (L). Data and BG represent measured spectra with the AmBe source and without the source. MC n_{GND} and MC $n_{1\mathrm{st}}$ indicate simulated spectra for neutrons with the ground state and 1st exited state of carbon. In a case of 1st exited state, 4438 keV γ-ray also emitted simultaneously.

$$R_{\mathrm{tail/peak}}(L) = \frac{\int_{4{,}750\ \mathrm{keV}}^{10{,}000\ \mathrm{keV}} \left\{ N(E_{\mathrm{vis}}, L) - N_{\mathrm{BG}}(E_{\mathrm{vis}}) \right\} dE_{\mathrm{vis}}}{\int_{4{,}321\ \mathrm{keV}}^{4{,}536\ \mathrm{keV}} \left\{ N(E_{\mathrm{vis}}, L) - N_{\mathrm{BG}}(E_{\mathrm{vis}}) \right\} dE_{\mathrm{vis}}}, \tag{2}$$

where $N(E_{\rm vis}, L)$ is the event rate for distance L and $E_{\rm vis}$ bin, and $N_{\rm BG}(E_{\rm vis})$ are the background rates for the $E_{\rm vis}$ bin. $R_{\rm tail/peak}$ as a function of L is shown in Figure 6. $R_{\rm n0/n1}$ is measured to be $0.68 \pm 0.01_{\rm stat.} \pm 0.05_{\rm syst.}$, by reproducing the $R_{\rm tail/peak}$ data distribution with that of simulation. The best fit value of $R_{\rm n1/n0}$ was determined with a minimum $\chi^2/dof = 9.46/9$.

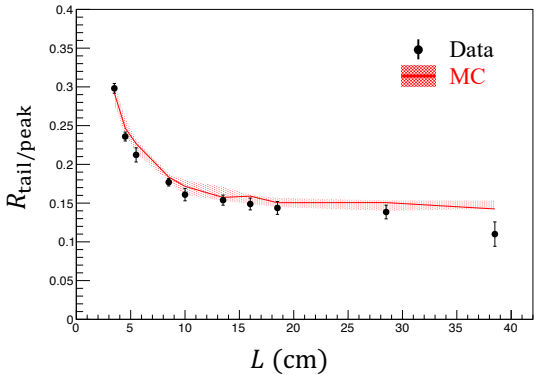

Figure 6: Black dots are data. Red line is the simulation with best fit of neutron emission ratio of $n_{\rm GND}$ to $n_{\rm 1st}$ with γ-ray emission. The red band shows a total systematic uncertainty, where a difference of cross section models for neutron interaction is a dominant contribution in this study.

4. Discussion and Conclusion

The measured emission parameters of neutrons and γ-ray are summarized in Table 1. Based on this information, we deduced the emission rates of neutrons from the AmBe source, that is, $n_{\rm 1st}$, $n_{\rm GND}$ and $n_{\rm 2nd}$. The $n_{\rm 1st}$ emission rate is assumed to be equal to S_γ. Second, the $n_{\rm GND}$ emission rate

Table 1: Summary of measured emission rate and ratio for the AmBe source.

Neutron yield	$S_{\rm n} = 236.8 \pm 5.0\ n \cdot {\rm s}^{-1}$
Intensity of 4438 keV γ emission	$S_\gamma = 110.1 \pm 15.5\ \gamma \cdot {\rm s}^{-1}$
Emission ratio of $n_{\rm GND}$ to $n_{\rm 1st}$	$R_{\rm n0/n1} = 0.68 \pm 0.01_{\rm stat.} \pm 0.05_{\rm syst.}$

is calculated by using $R_{\rm n0/n1} \cdot S_\gamma$ and is found to be $74.9 \pm 11.9\ n \cdot {\rm s}^{-1}$. Finally, the $n_{\rm 2nd}$ emission rate is estimated to be $51.8 \pm 17.2\ n \cdot {\rm s}^{-1}$ as the subtraction of $n_{\rm GND}$ and $n_{\rm 1st}$ emission rates from neutron yields S_γ. The results are consistent with the expectations for the $n_{\rm GND}$ and $n_{\rm 2nd}$ emission rates of $59.0 \pm 1.3\ n \cdot {\rm s}^{-1}$ ($n_{\rm GND}$) and $54.2 \pm 1.1\ n \cdot {\rm s}^{-1}$ ($n_{\rm 2nd}$), respectively. These expectations are given by our neutron energy spectrum model and the measured total neutron yield. As described above, our method successfully determines the emission rates of $n_{\rm GND}$, n1st, and $n_{\rm 2nd}$.

AmBe, which emits neutrons accompanied by γ-rays, is widely used to calibrate neutron detectors. We examined the characteristics of our AmBe source experimentally. These results are reasonably consistent with the expectations of our neutron spectrum model. The characteristics of the AmBe source can be understood by integrating the experimental measurement of the emission ratio of neutrons and the modeled energy spectra. Thus, these will contribute to the general use of AmBe sources, such as in measurements and calibrations for antineutrino physics experiments.

Acknowledgments

This work was partially supported by the joint research program of the Institute for Cosmic Ray Research (ICRR) at The University of Tokyo. This work was supported by the Neutron Measurement Consortium for Underground Physics, JSPS KAKENHI Grant Grants, Grant-in-Aid for Scientific Research (C) [grant number 20K03998], and Grant-in-Aid for Scientific Research on Innovative Areas [grant number 19H05808].

References

[1] Super-Kamiokande collaboration, *Search for Astrophysical Electron Antineutrinos in Super-Kamiokande with 0.01% Gadolinium-loaded Water*, *Astrophys. J. Lett.* **951** (2023) L27 [2305.05135].

[2] Super-Kamiokande collaboration, *Evaluation of neutron tagging efficiency for SK-Gd experiment*, *PoS* **ICHEP2022** (2022) 1178.

[3] H. Ito, K. Wada, T. Yano, Y. Hino, Y. Ommura, M. Harada et al., *Analyzing the neutron and γ-ray emission properties of an americium-beryllium tagged neutron source*, 2304.12153.

[4] A. Vijaya and A. Kumar, *The neutron spectrum of Am-Be neutron sources*, *Nucl. Instrum. Meth.* **111** (1973) 435.

[5] F. De Guarrini and R. Malaroda, *Two different technique measurements of the neutron spectrum of an Am-Be source*, *Nucl. Instrum. Meth.* **92** (1971) 277.

[6] E.A. Lorch, *Neutron Spectra of ^{214}Am/B, ^{241}Am/Be, ^{241}Am/F, ^{242}Cm/Be, ^{238}Pu/^{13}C and ^{252}Cf isotopic neutron sources*, *Int. J. Appl. Radiat. Isot.* **24** (1973) 585.

[7] K. Geiger and L. Van Der Zwan, *Radioactive neutron source spectra from 9Be(α, n) cross section data*, *Nucl. Instrum. Meth.* **131** (1975) 315.

[8] *Reference neutron radiations Part 1: Characteristics and methods of production, ISO 8529-1:2001(E)*, International Organization for Standardization (2001).

[9] M. Kostal et al., *Validation of heavy water cross section using ambe neutron source*, *EPJ Web Conf.* **239** (2020) 18008.

[10] T.K. Eriksen et al., *Improved precision on the experimental $E0$ decay branching ratio of the Hoyle state*, *Phys. Rev. C* **102** (2020) 024320 [2007.15374].

[11] H. Harano, T. Matsumoto, T. Shimoyama, Y. Sato, A. Uritani, Y. Hino et al., *Convenient method of relative calibration of the neutron source emission rate between different source types*, *IEEE Trans. Nucl. Sci.* **53** (2006) 1413.

[12] Z. Janout, S. Pospíšil and M. Vobecký, *Observation of a Doppler broadening of the 4438 keV gamma-line of ^{12}C in processes ^{12}C(n, n'γ)^{12}C and ^{9}Be(α, nγ)^{12}C*, *J. Radioanal. Chem.* **56** (1980) 71.